Chinese Journal of Natural Medicines

Anti-cancer and anti-inflammatory effects of flavan-4-ol and flavan glycosides from the roots of *Pronephrium penangianum*

Feibing Huang, Yong Yang, Qingling Xie, Hanwen Yuan, Muhammad Aamer, Yuqing Jian, Ye Zhang, Wei Wang

Citation: Feibing Huang, Yong Yang, Qingling Xie, Hanwen Yuan, Muhammad Aamer, Yuqing Jian, Ye Zhang, Wei Wang, Anti-cancer and anti-inflammatory effects of flavan-4-ol and flavan glycosides from the roots of *Pronephrium penangianum*, Chinese Journal of Natural Medicines, 2025, 23(5), 593-603. doi: 10.1016/S1875-5364(25)60814-4.

View online: https://doi.org/10.1016/S1875-5364(25)60814-4

Chinese Journal of Natural Medicines 23 (2025) 593-603

Contents lists available at ScienceDirect

Chinese Journal of Natural Medicines

journal homepage: www.cjnmcpu.com/

Original article

Anti-cancer and anti-inflammatory effects of flavan-4-ol and flavan glycosides from the roots of *Pronephrium penangianum*

Feibing Huang[a], Yong Yang[a], Qingling Xie[a], Hanwen Yuan[a], Muhammad Aamer[a,c], Yuqing Jian[a,*], Ye Zhang[b], Wei Wang[a,*]

[a] *TCM and Ethnomedicine Innovation & Development International Laboratory, Innovative Materia Medica Research Institute, School of Pharmacy, Hunan University of Chinese Medicine, Changsha 410208, China*

[b] *Shenzhen Futian District Maternity & Child Healthcare Hospital, Shenzhen 518000, China*

[c] *H. E. J. Research Institute of Chemistry, International Center for Chemical and Biological Sciences, University of Karachi, Karachi-75270, Pakistan*

ARTICLE INFO

Article history:
Received 6 August 2024
Revised 25 September 2024
Accepted 6 October 2024
Available online 20 May 2025

Keywords:
Pronephrium penangianum
Tujia ethnomedicine
Jixueqi
Flavan-4-ol and Flavan glycosides
Anti-cancer
Anti-inflammatory

ABSTRACT

Five new flavan-4-ol glycosides jixueqiosides A-E (**1**–**5**) and two new flavan glycosides jixueqiosides F and G (**6** and **7**), along with twelve known flavan-4-ol glycosides (**8**–**19**), were isolated from the roots of *Pronephrium penangianum*. Comprehensive spectral analyses, X-ray single-crystal diffraction, and theoretical electronic circular dichroism (ECD) calculations established structures and absolute configurations. A single crystal structure of flavan-4-ol glycoside (**14**) was reported for the first time, while the characteristic ECD and NMR data for all isolated flavan-4-ol glycosides (**1**–**5** , **8**–**19**) were analyzed, establishing a set of empirical rules. Activity screening of these isolates showed that **8** and **9** could inhibit the proliferation of MDA-MB-231 and MCF-7 cells with IC_{50} values of 7.93 ± 2.85 μmol·L^{-1} and 5.87 ± 1.58 μmol·L^{-1} (MDA-MB-231), and 2.21 ± 1.38 μmol·L^{-1} and 3.52 ± 1.55 μmol·L^{-1} (MCF-7), respectively. Western blotting and flow cytometry analyses demonstrated that **8** and **9** dose-dependently induced apoptosis in MDA-MB-231 cells by up-regulating BAX, activating caspase-3 and down-regulating BCL-2. Additionally, compound **8** affected autophagy-related proteins, increasing the ratio of LC3-II/LC3-I and Beclin-1 levels to inhibit MDA-MB-231 cell proliferation. Moreover, anti-inflammatory studies indicated that **2**, **3**, **7**, **13**, **14,** and **18** moderately inhibited tumor necrosis factor-α (TNF-α), interleukin-6 (IL-6), and nitric oxide (NO) release.

1. Introduction

Pronephrium penangianum (Hook.) Holtt. is a fern belonging to the Thelypteridaceae family, widely distributed across southern China [1]. The Tujia minority population has assigned this fern several vernacular names, including "jixueqi", "jixuelian", "huoxuelian", and "fengweiqi". It is commonly utilized as a Tujia ethnomedicine for treating menstrual irregularities, traumatic injury, and rheumatism [2, 3]. Additionally, *P. penangianum* has been classified in the same order (Polypodiales, Filicales) as the traditional Chinese medicine (TCM) species *Cibotium barometz* (gou ji), *Cyrtomium fortunei* (guan zhong), and *Pyrrosia lingua* (shi wei), prompting further investigation into this intriguing taxonomic association [1]. Literature review indicates that flavan-4-ol glycosides, the primary constituents of *P. penangianum*, have been reported in only four plant species: *P. penangianum* [4], *P. triphyllum* [5, 6], *P. gymnopteridifrons* [7], and *Glaphyropteridopsis erubescens* [8]. *P. penangianum* represents one of the richest sources of flavan-4-ol glycosides. Furthermore, previous studies have demonstrated its pharmacological potential, encompassing anti-inflammatory, anti-tumor, neuroprotective, antioxidant, anti-benign prostatic hyperplasia, anti-fibrotic, and analgesic effects [3].

While numerous flavan-4-ol glycosides have been identified in *P. penangianum*, their electronic circular dichroism (ECD) and nuclear magnetic resonance (NMR) data characteristics have not been systematically analyzed. This study examines the ECD and NMR characteristics data of isolated flavan-4-ol glycosides, establishing a set of empirical rules to facilitate rapid identification of planar and relative structural configurations. Additionally, natural products serve as valuable sources of drugs with diverse bioactivities [9]. Consequently, all compounds were evaluated for their anti-cancer and anti-inflammatory activities *in vitro*. Compounds **8** and **9** demonstrated significant inhibitory effects on breast cancer cell proliferation (MDA-MB-231 and MCF-7), suggesting their potential as anti-breast cancer drug candidates.

2. Results and discussion

Compound **1** was isolated as an amorphous white powder. Its molecular formula was determined by high-resolution electrospray ionization mass spectrometry (HR-ESI-MS) (*m/z* 511.1575 $[M + Na]^+$, Calcd. for $C_{25}H_{28}O_{10}Na^+$, 511.1580). The ultraviolet (UV) spectrum exhibited maximum absorptions at 206, 226, and 275 nm. The infrared (IR) spectrum revealed characteristic ab-

* Corresponding author.
E-mail addresses: cpujyq2010@163.com (Y. Jian); wangwei402@hotmail.com (W. Wang)

https://doi.org/10.1016/S1875-5364(25)60814-4

sorption peaks at 3411, 1737, 1613, and 1518 cm^{-1} for hydroxyl, carbonyl, and phenyl functionalities. The ^1H NMR spectrum (Table 1) displayed characteristic signals for one *para*-substituted phenyl group at δ_H 7.34 (H-2'/6') and 6.96 (H-3'/5'), (each 2H, d, J = 8.4 Hz), three methyls at δ_H 2.14 (6-CH_3), 2.11 (COCH_3) and 2.06 (8-CH_3) (each 3H, s), one anomeric proton at δ_H 4.37 (1H, d, J = 7.2 Hz, H-1'') as well as signals for glucose moiety at δ_H 3.42 - 4.44 (H-2''–H-6''). The ^{13}C NMR spectrum (Table 2) indicated the presence of a carbonyl group at δ_C 172.8 ($COCH_3$), one *para*-substituted phenyl group [δ_C 158.4 (C-4'), 133.4 (C-1'), 128.6 (C-2'/6'), and 116.1 (C-3'/5')], one fully substituted phenyl group [δ_C 155.0 (C-7), 153.4 (C-9), 152.5 (C-5), 113.7 (C-10), 111.3 (C-6), and 110.0 (C-8)], and two aromatic methyl groups δ_C 9.3 (6-CH_3) and 8.8 (8-CH_3) in the aglycon.

Three spin systems (H-2'/6' to H-3'/5', H-2 to H-4 and H-1'' to H-6'') were identified based on the ^1H–^1H COSY spectrum (Fig. 2). The heteronuclear multiple bond (HMBC) correlations of H-6' with C-2'/C-4' and H-5' with C-1'/C-3' indicated the presence of a *para*-substituted phenyl group (Fig. 2). Additionally, the HMBC correlations of H-4 (δ_H 5.01) and C-2/C-9 (δ_C 78.3/153.4), H-3a/3b (δ_H 2.17/2.56) and C-10 (δ_C 113.7), H-6 (δ_H 2.14, 6-CH_3) and C-5/C-7 (δ_C 152.5/155.0), and H-8 (δ_H 2.06, 8-CH_3) and C-7/C-9 (δ_C 155.0/153.4), confirmed the existence of a 6,8-dimethyl chromanol moiety. Moreover, the HMBC correlations of H-2 (δ_H 4.85) with C-2'/C-6' (δ_C 128.6) further supported that the skeleton of **1** was 6,8-dimethyl-2-phenyl-chromanol. The HMBC correlations of H-1'' (δ_H 4.37) with C-5 (δ_C 152.5) and H-4 (δ_H 5.01) with C-2'' (δ_C 86.8) suggested that the glucose moiety has two binding sites to the aglycon, with C-1'' attached to C-5 and C-2'' attached to C-4 through an oxygen bridge, respectively. Consequently, C-5, C-10, C-4, C-2'' and C-1'' formed a dioxepane ring. Furthermore, the correlations of H-6''a (δ_H 4.29) and H-6''b (δ_H 4.44) as well as a methyl signal (δ_H 2.11) with the carbonyl carbon (δ_C 172.8) indicated that 6''-OH of the glucose moiety was acetylated. Comparison of the NMR data of **1** with those of abacopterin A (**8**) [10] revealed that their planar structures were quite similar. The primary difference between **1** and abacopterin A was that **1** has one less 4'-methyl group than abacopterin A. After acid hydrolysis and derivatization of **1**, analytical high-performance liquid chromatography (HPLC) analysis confirmed the presence of a D-glucose unit [11]. The β-configuration of D-glucose was determined by the coupling constants of the anomeric proton signals at δ_H 4.37 (1H, d, $^3J_{H1''\text{-}H2''}$ = 7.2 Hz, H-1'').

In the rotating frame Overhauser effect spectroscopy (ROESY) spectrum, correlations between H-2 to H-4 and H-4 to H-2'' indicated that H-2 and H-4 were positioned in the same orientation within the dihydropyran ring of **1** (Fig. 3). Moreover, the strong agreement between the calculated ECD spectrum (Fig. S3) of 2*S*, 4*S*-**1** and experimental data confirmed the absolute configuration of compound **1**. Consequently, the structure of compound **1** was determined to be (2*S*, 4*S*)-6,8-dimethyl-7,4'-dihydroxyl-4,2''-oxidoflavan-5-*O*-β-D-6-*O*-acetyl-glucopyranoside, and named jixueqioside A.

Compound **2** was isolated as an amorphous white powder. Its molecular formula was determined through HRESIMS (*m/z* 511.1575 $[M + Na]^+$, Calcd. for $C_{25}H_{28}O_{10}Na^+$, 511.1580). The NMR, UV, and IR spectra of **2** exhibited similarities to those of the known compound **11** [12], indicating structural resemblance between the two compounds. Comparison of the ^1H and ^{13}C NMR spectra of **2** with **11** revealed the absence of an oxygenated methyl group at C-4' in **2**. The absolute configuration of **2** was established as 2*S* and 4*R* based on nuclear Overhauser effect (NOE) correlations (H-2 to H-3b and H-4 to H-3a) (Fig. 3) and ECD calculation (Fig. S3). Acid hydrolysis and derivatization of **2**, followed by analytical HPLC analysis, confirmed the presence of a D-glucose unit [11]. The β-configuration of D-glucose was determined by the coupling constants of the anomeric proton signals at δ_H 5.12 (1H, d, $^3J_{H1''\text{-}H2''}$ = 8.4 Hz, H-1''). Consequently, the structure of **2** was elucidated as (2*S*,4*R*)-6,8-dimethyl-7,4'-dihydroxyl-4,2''-oxidoflavan-5-*O*-β-D-6-*O*-acetyl-glucopyranoside, and named jixueqioside B.

Compound **3** was isolated as an amorphous white powder. Its molecular formula was determined through HRESIMS (*m/z* 501.1758 $[M - H]^-$, Calcd. for $C_{26}H_{29}O_{10}^-$, 501.1761). The ^1H and ^{13}C NMR spectra of **3** were analogous to those of **2**. The primary distinctions between **3** and **2** were the presence of an oxygen-

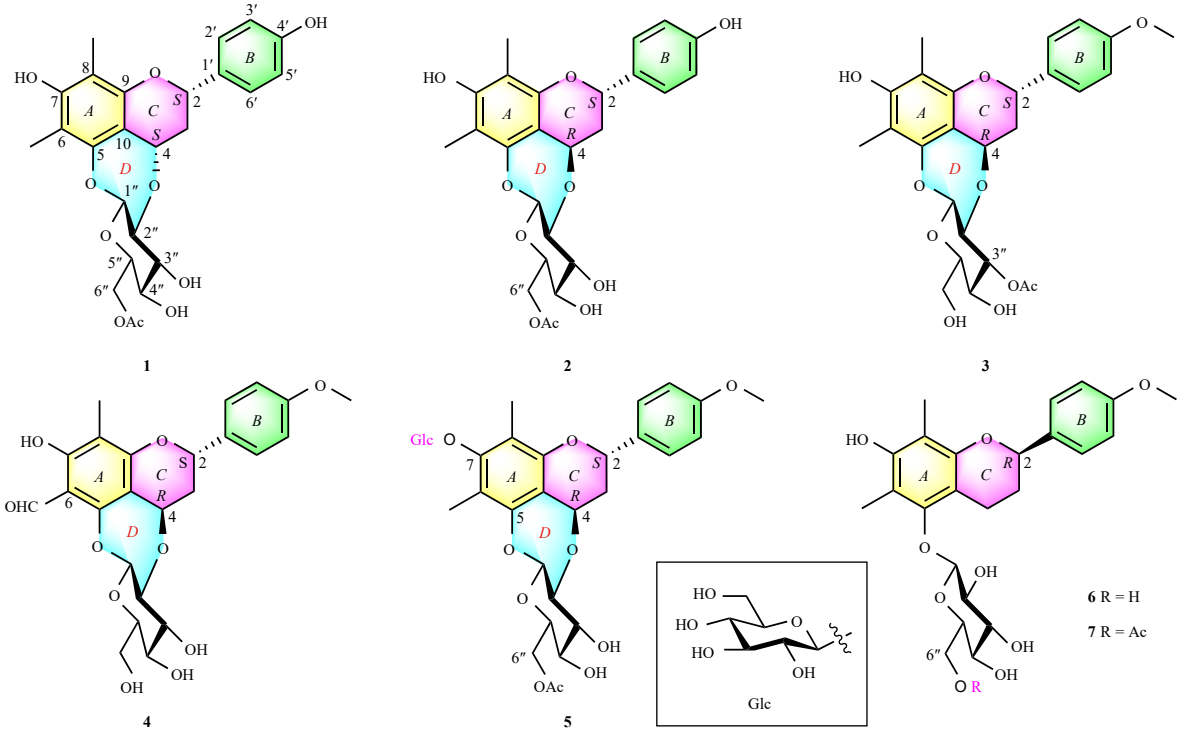

Fig. 1 Structures of compounds **1**–**7**.

Table 1 ^{1}H NMR (600 MHz) data for **1**–**7** in CD_3OD (δ in ppm, mult., J in Hz)

No.	1	2	3	4	5	No.	6	7
2	4.85, dd (12.0, 1.2)	4.82, dd (12.6, 1.2)	4.64, dd (12.0, 1.8)	5.04, dd (12.6, 1.2)	4.88, dd (12.6, 1.2)	2	4.95, dd (9.6, 1.8)	4.94, dd (9.6, 1.8)
3a	2.17, ddd (13.2, 12.0, 10.2)	2.00, ddd (14.4, 12.6, 4.2)	1.99, ddd (14.4, 12.0, 4.2)	2.10, ddd (14.4, 12.6, 4.2)	2.00, ddd (14.4, 12.6, 4.2)	3a	1.83, m	1.80, m
3b	2.56, ddd (13.2, 7.8, 1.2)	2.29, dt (14.4, 1.2)	2.12, dt (14.4, 1.8)	2.36, dt (14.4, 1.2)	2.32, dt (14.4, 1.2)	3b	2.12, m	2.10, m
4	5.01, dd (10.2, 7.8)	5.10, dd (4.2, 1.2)	5.06, dd (4.2, 1.8)	5.15, dd (4.2, 1.2)	5.11, dd (4.2, 1.2)	4a	2.81, ddd (17.0, 5.4, 3.6)	2.74, ddd (17.0, 5.4, 3.6)
6-CH_3	2.14, s	2.07, s	2.14, s	2.01, s	2.23, s	4b	2.98, ddd (17.0, 11.3, 6.0)	2.90, ddd (17.0, 11.3, 6.0)
8-CH_3	2.06, s	2.04, s	2.06, s	-	2.17, s	6-CH_3	2.19, s	2.19, s
8-CHO	-	-	-	10.2, s	-	8-CH_3	2.05, s	2.05, s
2'	7.34, d (8.4)	7.32, d (8.4)	7.34, d (9.0)	7.43, d (9.0)	7.43, d (8.4)	2'	7.33, d (9.0)	7.33, d (8.4)
3'	6.96, d (8.4)	6.81, d (8.4)	6.96, d (8.4)	6.97, d (8.4)	6.95, d (8.4)	3'	6.91, d (8.4)	6.91, d (8.4)
5'	6.96, d (8.4)	6.81, d (8.4)	6.96, d (8.4)	6.97, d (8.4)	6.95, d (8.4)	5'	6.91, d (8.4)	6.91, d (8.4)
6'	7.34, d (8.4)	7.32, d (8.4)	7.34, d (9.0)	7.43, d (9.0)	7.43, d (8.4)	6'	7.33, d (9.0)	7.33, d (8.4)
4'-OCH_3	-	-	3.82, s	3.83, s	3.81, s	4'-OCH_3	3.79, s	3.80, s
1''	4.37, d (7.2)	5.12, d (8.4)	5.22, d (8.4)	5.36, d (8.4)	5.16, d (8.4)	1''	4.58, d (7.8)	4.55, d (7.8)
2''	3.42, m	3.30, m	3.45, overlapped	3.44, overlapped	3.31, m	2''	3.49, t (9.0)	3.47, t (8.8)
3''	3.45, m	3.59, t (9.0)	5.13, t (9.6)	3.44, overlapped	3.60, m	3''	3.41, t (9.0)	3.40, t (8.8)
4''	3.45, m	3.19, m	3.37, t (9.0)	3.23, t (9.6)	3.18, m	4''	3.37, t (9.0)	3.35, t (8.8)
5''	3.60, ddd (9.6, 5.4, 2.0)	3.54, m	3.45, overlapped	3.66, overlapped	3.54, m	5''	3.14, m	3.31, overlapped
6''a	4.29, dd (12.0, 5.4)	4.18, dd (12.0, 6.0)	3.68, dd (12.0, 6.0)	3.66, overlapped	4.22, dd (12.0, 6.0)	6''a	3.68, dd (12.0, 6.0)	4.28, dd (11.8, 6.0)
6''b	4.44, dd (12.0, 1.8)	4.45, dd (12.0, 1.8)	3.89, dd (12.0, 1.8)	3.89, dd (12.0, 1.8)	4.43, dd (12.0, 1.8)	6''b	3.81, dd (12.0, 2.4)	4.33, dd (11.8, 2.4)
-COCH_3	2.11, s	2.07, s	2.08, s	-	2.07, s	-COCH_3	-	1.98, s
1'''	-	-	-	-	4.64, d (7.8)		-	-
2'''	-	-	-	-	3.52, m		-	-
3'''	-	-	-	-	3.43, m		-	-
4'''	-	-	-	-	3.38, m		-	-
5'''	-	-	-	-	3.14, m		-	-
6'''a	-	-	-	-	3.66, dd (12.0, 5.4)		-	-
6'''b	-	-	-	-	3.77, dd (12.0, 2.4)		-	-

Table 2 ^{13}C NMR (150 MHz) data for **1**–**7** in CD_3OD

Positon	1	2	3	4	5	6	7
2	78.3 d	74.9 d	75.0 d	76.1 d	74.8 d	78.4 d	78.4 d
3	38.9 t	38.3 t	38.7 t	37.3 t	38.1 t	31.1 t	31.1 t
4	74.5 d	67.1 d	67.0 d	66.1 d	66.9 d	22.0 d	21.9 d
5	152.5 s	151.0 s	151.0 s	157.6 s	151.4 s	152.5 s	152.1 s
6	111.3 s	110.9 s	111.3 s	109.7 s	117.0 s	111.5 s	111.4 s
7	155.0 s	156.1 s	156.2 s	162.5 s	156.2 s	153.1 s	153.1 s
8	110.0 s	109.4 s	109.5 s	109.6 s	118.3 s	110.3 s	110.4 s
9	153.4 s	152.9 s	152.8 s	162.0 s	152.9 s	152.3 s	152.5 s
10	113.7 s	105.3 s	104.9 s	104.8 s	109.6 s	110.0 s	110.0 s
6-CH_3	9.3 q	9.3 q	9.5 q	7.1 q	10.5 q	10.3 q	10.2 q
8-CH_3	8.8 q	8.6 q	8.6 q	195.2 q	10.3 q	8.8 q	8.8 q
1'	133.4 s	133.6 s	134.4 s	133.4 s	134.5 s	136.1 s	136.0 s
2'	128.6 d	128.7 d	128.4 d	128.8 d	128.6 d	128.1 d	128.1 d
3'	116.1 d	116.1 d	114.9 d	114.9 d	116.1 d	114.7 d	114.7 d
4'	158.4 s	158.2 s	161.0 s	161.2 s	160.9 s	161.0 s	161.0 s
5'	116.1 d	116.1 d	114.9 d	114.9 d	116.1 d	114.7 d	114.7 d
6'	128.6 d	128.7 d	128.4 d	128.8 d	128.6 d	128.1 d	128.1 d
4'-OCH_3	-	-	55.7 q	55.8 q	55.7 q	55.7 q	55.7 q
1''	103.2 d	102.3 d	102.3 d	102.5 d	102.4 d	106.0 d	105.7 d
2''	86.8 d	75.7 d	74.1 d	79.1 d	75.9 d	75.8 d	75.7 d
3''	75.6 d	76.4 d	77.4 d	76.2 d	76.3 d	77.9 d	77.9 d
4''	71.2 d	71.6 d	69.6 d	71.3 d	71.7 d	71.7 d	71.8 d
5''	76.4 d	76.0 d	78.8 d	76.5 d	76.1 d	77.9 d	75.3 d
6''	64.6 t	64.5 t	62.6 t	62.6 t	64.6 t	62.8 t	64.3 t
-$COCH_3$	172.8 s	172.7 s	172.3 s	-	172.8 s	-	172.6 s
-$COCH_3$	20.7 q	20.7 q	21.1 q	-	20.8 q	-	20.8 q
1'''	-	-	-	-	105.6 d	-	-
2'''	-	-	-	-	75.8 d	-	-
3'''	-	-	-	-	78.0 d	-	-
4'''	-	-	-	-	71.7 d	-	-
5'''	-	-	-	-	78.0 d	-	-
6'''	-	-	-	-	62.8 t	-	-

ated methyl group (δ_H 3.82, δ_C 55.7) attached to C-4' of **3** and the acetylation of 3''-OH in the glucose moiety unit. This was further corroborated by the correlation of H-3'' (δ_H 5.13) with the carbonyl carbon (δ_C 172.3) in the HMBC spectrum (Fig. 2). Additionally, acid hydrolysis and derivatization of **3** with hydrochloric acid (HCl) yielded D-glucose, which was identified by analytical HPLC [11]. The *β*-configuration of the glycosidic bond was inferred from the value of the anomeric proton signals at δ_H 5.22 (1H, d, $^3J_{H1''\text{-}H2''}$ = 8.4 Hz, H-1''). The absolute configuration of **3** was established as 2*S* and 4*R* based on NOE correlations (Fig. S36) and ECD calculation (Fig. S3). Consequently, the structure of **3** was elucidated as (2*S*,4*R*)-6,8-dimethyl-7-hydroxyl-4'-methoxy-4,2''-oxidoflavan-5-*O*-*β*-D-3-*O*-acetyl-glucopyranoside, and named jixueqioside C.

Compound **4** was isolated as an amorphous white powder. Its molecular formula was determined by HRESIMS (*m/z* 473.1451

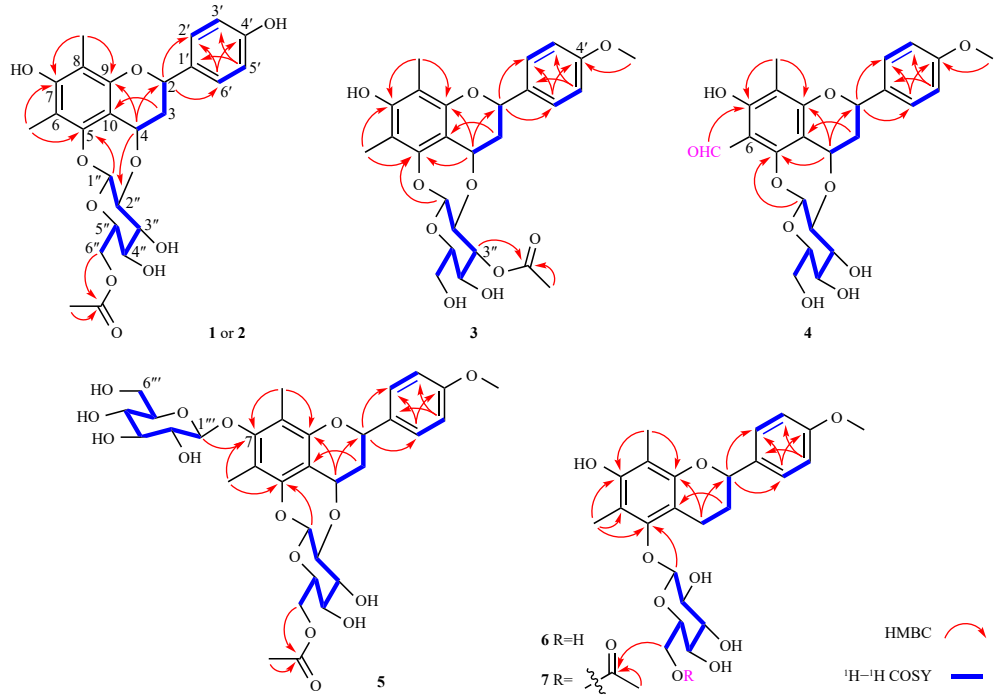

Fig. 2 Key $^{1}H–^{1}H$ COSY and HMBCs of compounds **1**–**7**.

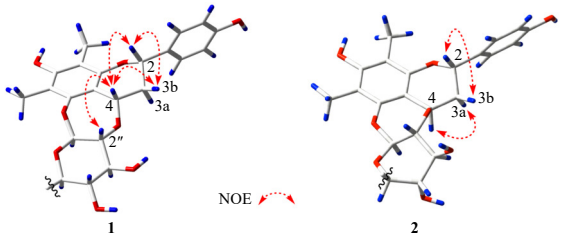

Fig. 3 Key ROESY correlation of compounds **1** and **2**.

[M − H]$^-$, Calcd. for $C_{24}H_{25}O_{10}^-$, 473.1448). The HRESIMS spectrum of **4** also exhibited fragment ions at *m/z* 311.0916 [M − H − $C_6H_{10}O_5$]$^-$, indicating the presence of a glucose moiety. Acid hydrolysis, derivatization of **4**, and subsequent analytical HPLC analysis confirmed the presence of a D-glucose unit [11]. The *β*-configuration of D-glucose was established by the coupling constants of the anomeric proton signals at δ_H 5.36 (1H, d, $^{3}J_{H1''\text{-}H2''}$ = 8.4 Hz, H-1''). Comparison of NMR spectral data with those of **3** revealed that the methyl at C-6 was replaced by an aldehyde group (δ_H 10.2, δ_C 195.2), and the acetyl group was absent in **4**. In the HMBC spectrum (Fig. 2), correlations between the protons of methyl (δ_H 2.01) with C-7 (δ_C 162.5), C-9 (δ_C 162.0), and -CHO (δ_H 10.2) with C-7 (δ_C 162.5) indicated the methyl group at C-8 and -CHO at C-6. The NOE correlation between -CHO (δ_H 10.2) and H-1'' (δ_H 5.36) further supported the position of -CHO. The configuration of **4** was determined as 2*S* and 4*R* based on NOE correlations (Fig. S47) and ECD calculations (Fig. S3). Consequently, the structure of **4** was elucidated as (2*S*,4*R*)-6-aldehyde-8-methyl-7-hydroxyl-4'-methoxy-4,2''-oxidoflavan-5-*O*-*β*-D-glucopyranoside, and named jixueqioside D.

Compound **5** was isolated as white needles. Its molecular formula was determined by HRESIMS (*m/z* 687.2247 [M + Na]$^+$, Calcd. for $C_{32}H_{40}O_{15}Na^+$, 687.2265). Comparison of the ^{1}H and ^{13}C NMR spectra of **5** with those of **14** revealed that structure **5** was similar to abacopterin I (**14**) [13], differing only in the absence of an acetyl group. The configurations at C-2 and C-4 were confirmed as 2*S* and 4*R* based on NOE correlations and ECD calculations (Fig. S3) of **5**. Furthermore, comparison of the spectral data of **5** with **14** confirmed that both compounds shared the same configuration at C-2 and C-4. Additionally, X-ray data (Fig. 4) for abacopterin I (**14**) was obtained for the first time, supporting the confirmation of the flavan-4-ol configuration. Acid hydrolysis and derivatization of **5** with HCl yielded D-glucose, which was further identified by analytical HPLC [11]. The *β*-configuration of the glycosidic bonds was deduced from the anomeric proton signals at δ_H 5.16 (1H, d, $^{3}J_{H1''\text{-}H2''}$ = 8.4 Hz, H-1'') and 4.64 (1H, d, $^{3}J_{H1'''\text{-}H2'''}$ = 7.8 Hz, H-1'''). Consequently, compound **5** was determined to be (2*S*,4*R*)-4'-methoxy-6,8-dimethyl-4,2''-oxidoflavan-5-*O*-*β*-D-6-*O*-acetyl-glucopyranoside-7-*O*-*β*-D-glucopyranoside and named jixueqioside E.

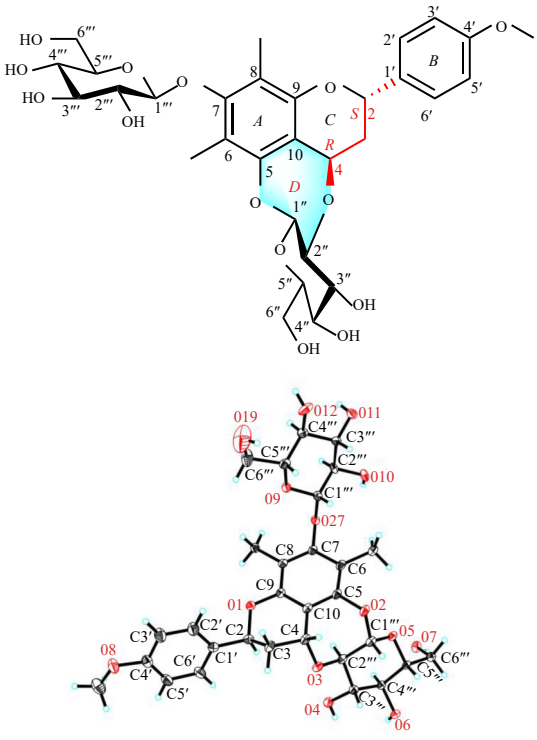

Fig. 4 Structure of **14** and its single-crystal X-ray structure.

Compound **6** was isolated as a colorless amorphous powder. Its molecular formula was determined by HR-ESI-MS (*m/z* 461.1814 [M − H]$^-$, Calcd. for $C_{24}H_{29}O_9^-$, 461.1812). The HR-ESI-MS spectrum of **6** also displayed fragment ions at *m/z* 299.1286 [M − H − $C_6H_{10}O_5$]$^-$, indicating the presence of a glucose moiety. Acid hydrolysis and derivatization of **6**, followed by analytical HPLC analysis, confirmed the presence of a D-glucose unit [11]. The *β*-configuration of D-glucose was established based on the coupling constants of the anomeric proton signals at δ_H 4.58 (1H, d, $^3J_{H1''\text{-}H2''}$ = 7.8 Hz, H-1''). NMR spectra (Tables 1 and 2) of **6** in CD_3OD revealed a set of AA'XX' systems at δ_H 7.33 (2H, d, *J* = 9.0 Hz), δ_C 128.1 × 2 and δ_H 6.91 (2H, d, *J* = 8.4 Hz), δ_C 114.7 × 2, an oxygenated methine at δ_H 3.79 (3H, s), δ_C 55.7, two singlet methyls at δ_H 2.05 (3H, s), δ_C 8.8 and δ_H 2.19 (3H, s), δ_C 10.3, an anomeric signal at δ_H 4.58 (1H, d, *J* = 7.8 Hz), δ_C 106.0, and a series of signals corresponding to the glucose moiety at δ_H 3.14-3.81, δ_C 62.8-77.9. These data suggest that compound **6** is likely a 6,8-dimethyl-2-phenyl-chromanol glycoside. The attachment of the glucose moiety at C-5 was confirmed by HMBC correlations (Fig. 2) between Glc-H-1'' (δ_H 4.58) and C-5 (δ_C 152.5), as well as ROESY correlations (Fig. S69) between Glc-H-1'' (δ_H 4.58) and Me-6 (δ_H 2.19) and H-4a (δ_H 2.81). The absolute configuration was determined to be *R* by comparing its experimental and calculated ECD curves (Fig. S3). Consequently, compound **6** was identified as (2*R*)-6,8-dimethyl-7-hydroxy-4'-methoxyflavan-5-*O*-*β*-D-glucopyranoside, and named Jixueqioside F.

Compound **7** was isolated as a colorless amorphous powder. Its molecular formula was determined by HR-ESI-MS (*m/z* 505.2051 [M + H]$^+$, Calcd. for $C_{26}H_{33}O_{10}^+$, 505.2074). The NMR spectroscopic data of **7** closely resembled those of **6** (Tables 1 and 2). The primary distinction between **7** and **6** was the acetylation of the 6''-OH of the glucose moiety in **7**, as confirmed by the HMBC correlations from H-6'' (δ_H 4.28 and 4.33) to C=O (δ_C 172.6), and a methyl (δ_H 1.98) to C=O (δ_C 172.6) (Fig. 2). The absolute configuration of C-2 in compound **7** was determined to be *R* by comparing its experimental and calculated ECD curves with those of **6** (Fig. S3). After acid hydrolysis and derivatization of **7**, analytical HPLC analysis revealed the presence of a D-glucose unit [11]. The *β*-configuration of D-glucose was established by the coupling constants of the anomeric proton signals at δ_H 4.55 (1H, d, $^3J_{H1''\text{-}H2''}$ = 7.8 Hz, H-1''). Consequently, compound **7** was characterized as (2*R*)-6,8-dimethyl-7-hydroxy-4'-methoxyflavan-5-*O*-*β*-D-6-*O*-acetyl-glucopyranoside, and named jixueqioside G.

In addition to the five new flavan-4-ol glycosides (**1**–**5**) and two rare 6,8-dimethyl-2-phenyl-chromanol glycosides (**6**–**7**) (Fig. 1), twelve known flavan-4-ol glycosides were isolated. These were identified as abacopterin A (**8**) [10], abacopterin C (**9**) [10], abacopterin E (**10**) [13], (2*S*, 4*R*)-6,8-dimethyl-7-hydroxy-4'-methoxy-4,2''-oxidoflavan-5-*O*-*β*-D-6''-*O*-acetyl-glycopyranoside (**11**) [12], eruberin A (**12**) [14], abacopterin F (**13**) [13], abacopterin I (**14**) [13], (2*S*,4*R*)-4'-methoxy-6-hydroxymethyl-8-methyl-4,2''-oxidoflavan-5,7-di-*O*-*β*-D-glucopyranoside (**15**) [7], triphyllin A (**16**) [13], eruberin B (**17**) [14], eruberin C (**18**) [14] and (2*S*,4*R*)-4,4'-dimethoxy-6-methoxymethyl-8-methyl-5,7-di-*O*-*β*-D-glucopyranoside (**19**) [7]. The identification was accomplished by comparing their NMR, HRESIMS, and ECD data (Fig. S2) with those of reported literature.

To date, twenty-six flavan-4-ol glycosides have been identified from four plant species: *P. penangianum* [4], *P. triphyllum* [5,6], *P. gymnopteridifrons* [7] and *G. erubescens* [8]. The majority of these compounds exist as glycosides and have been predominantly isolated from *P. penangianum*. The classification of flavan-4-ol glycosides is based on the position and number of linked glucose moieties or the presence of a dioxepane ring formed between the glucose and aglycone components. This investigation revealed nineteen flavan-4-ol glycosides from *P. penangianum*, including seven new compounds. The structures of all flavan-4-ol glycosides were determined through NMR data analysis, ECD calculations, and by comparing the spectral data with literature. Notably, this study presented a single crystal structure of a flavan-4-ol glycoside (**14**) for the first time. These compounds were categorized into closed and open D-ring subtypes based on their structural characteristics. The configurations of the flavan-4-ol aglycone moiety primarily manifest as two subtypes: (2*S*, 4*S*) and

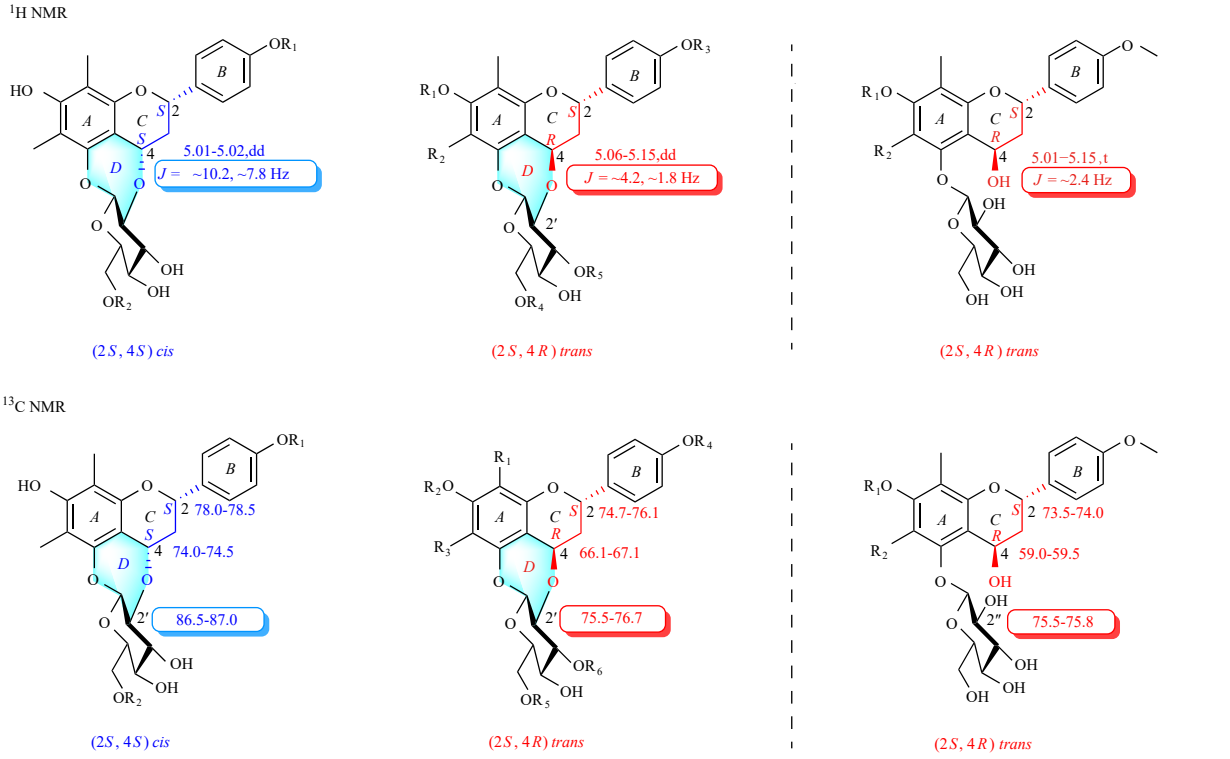

Fig. 5 The Key ^{1}H NMR (600 MHz) and ^{13}C NMR (150 MHz) data characterization of flavan-4-ols.

(2*S*, 4*R*).

A study [15] indicates that the ECD regulation of flavan-4-ols exhibits a negative cotton effect around 240 and 280 nm in the 2*S*, 4*S* configuration and a positive cotton effect around 240 and 280 nm in the 2*S*, 4*R* configuration. The ECD data for all compounds isolated in the present study (Figs. S2 and S3) align with these established guidelines.

Following the determination of the absolute configuration of the aforementioned compounds, the characteristic ^{1}H and ^{13}C NMR data for this class of compounds were systematically analyzed (Fig. 5, Tables S3 and S4). In the ^{1}H NMR spectra, the main differences are the coupling constants of H-3a/3b and H-4. Regarding the ^{13}C NMR data, it is feasible to ascertain whether the D-ring is open or closed, as well as the chiral carbon configurations of flavan-4-ols, based on the chemical shift values of C-2, C-3, and C-4. Notably, the comprehensive considertation of both ^{1}H and ^{13}C NMR data is more convincing.

Based on the activity screening results, compounds **8** and **9** demonstrated significant anti-breast cancer effects (Fig. 8), prompting further investigation into their mechanisms. Apoptosis, a fundamental and complex biological process, plays a crucial role in maintaining cellular homeostasis. Proteins from the BAX family, which promote apoptosis, and those from the BCL-2 family, which inhibit it, are recognized as key regulators of this cell death mechanism [16]. The BCL-2/BAX ratio serves as a biomarker for apoptosis induced in cancer cells by chemotherapy and radiation treatments. Disruption of the balance between BCL-2 and BAX alters mitochondrial membrane permeability (MMP), triggering the release of cytochrome c into the cytoplasm and ultimately increasing activated caspase-3 levels. In this study, compounds **8** and **9** significantly increased the apoptosis rate in MDA-MB-231 cells by reducing BCL-2 expression while enhancing BAX expression and activating caspase-3 (Figs. 6 and 7). Consequently, these compounds induce apoptosis in MDA-MB-231 cells through the mitochondrial apoptotic pathway.

Given the established correlation between autophagy and cancer, compound **8** was further examined for its effects on autophagy-related proteins. The levels of light chain 3 (LC3) were assessed *via* immunoblot analysis of MDA-MB-231 cells treated with **8**, allowing for the differentiation between cytoplasmic LC3-I and autophagosome-bound LC3-II. The conversion of LC3-I to LC3-II represents a crucial step in the autophagy process [17]. Western blotting analysis revealed a significant increase in lipidated LC3-II following treatment with varying concentrations of **8**. Additionally, the accumulation of Beclin 1, a key regulator of autophagosome formation, further indicated the activation of autophagy (Fig. 6).

Consequently, this study concludes that **8** appears to induce apoptosis and activate autophagy, ultimately inhibiting the proliferating cell nuclear antigen (PCNA) levels and affecting the proliferation of MDA-MB-231 cells.

3. Conclusions

In conclusion, the chemical investigation of *P. penangianum* yielded 19 compounds, comprising five new flavan-4-ol glycosides (**1**–**5**), two new flavan glycosides (**6**–**7**), and twelve known flavan-4-ol glycosides (**8**–**19**). All compounds shared a common 6,8-dimethyl chromanol moiety. Notably, these compounds have been identified in only a few plant species, and unlike previous discoveries with either 6-CH_3 or 8-CH_3 substitutions, flavan glycosides with methyl groups at both C-6 and C-8 positions are exceptionally rare in nature. Additionally, the X-ray single-crystal structure of one flavan-4-ol glycoside (**14**) was reported for the first time. Furthermor, all compounds underwent evaluation for anti-cancer and anti-inflammatory activities. Compounds **8** and **9** demonstrated significant activity against MDA-MB-231 and MCF-7 cells (Table 3). Their anti-proliferative mechanism on MDA-MB-231 cells was examined through Western blotting and flow cytometry analysis. Moreover, compounds **2**, **3**, **7**, **13**, **14**, and **18** exhibited moderate inhibition of tumor necrosis factor-α (TNF-α), interleukin-6 (IL-6), and nitric oxide (NO) release (Table 4). This study provides valuable insights into the configuration of flavan-4-ol glycoside structures and identifies flavan-4-ol glycosides as potential active constituents with anti-breast cancer properties.

4. Experimental

4.1. General procedures

Chemistry. The ECD spectra were recorded using a JASCO J1500 spectropolarimeter (JASCO Corporation, Japan). Optical rotations were measured with a Rudolph III-AUTOPOL polarimeter (Rudolph Research Analytical, USA). HRESIMS data were obtained on a Thermo Scientific Orbitrap Exploris 120 (Thermo Scientific, USA). Spectrophotometric analyses were conducted using a UV-1900i (Shimadzu, Japan). IR spectra were recorded on a Nicolet iS5 FT IR spectrometer (Thermo Scientific, USA) using KBr disks. ^{1}H and ^{13}C NMR spectra were acquired on a Bruker 600 MHz spectrometer (Bruker Corporation, Germany) in CD_3OD, with tetramethylsilane (TMS) as the internal standard. Preparative and semi-preparative HPLC were performed on an Agilent 1260 HPLC (Agilent Technologies, USA) utilizing a Comosil $5C_{18}$ MS-II (10.0 mm × 250 mm) column. Column chromatography was conducted using silica gel (100–200, 200–300 mesh, Qingdao Marine Chemical Co., Ltd., China) and MCI gel (75–150 μm, Mitsubishi Chemical Corporation, Japan). Fractions were monitored by TLC (GF 254, Qingdao Marine Chemical Co., Ltd., China), with spots visualized by heating silica gel plates sprayed with 10% H_2SO_4 in ethanol (EtOH).

Bioassays. Cell lines utilized in this study were obtained

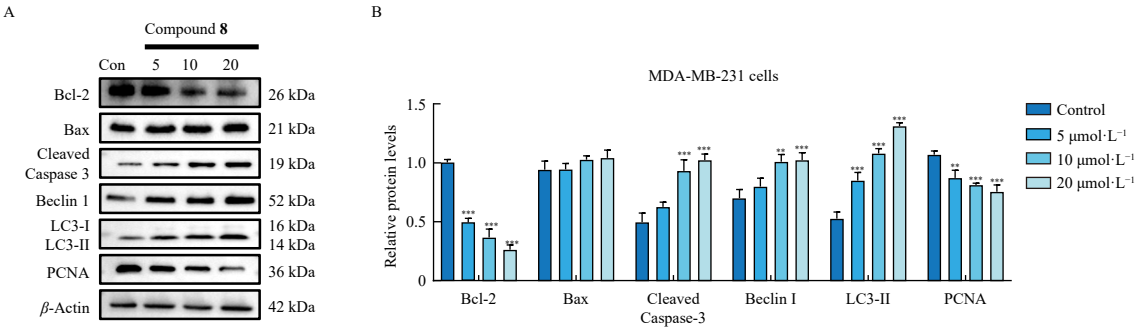

Fig. 6 Effect of compound **8** on the levels of apoptosis-associated, autophagy-related, and proliferation-related molecules in MDA-MB-231 cells. (A) Levels of BAX, BCL-2, Cleaved Caspase-3, Beclin 1, LC3-II, and PCNA in **8**-incubated MDA-MB-231 cells were examined using Western blotting. (B) Quantitative analysis of the protein levels indicated above. All data are represented as the average of three independent experiments ± SEM. $^{**}P < 0.01$; $^{***}P < 0.001$, *vs* control group.

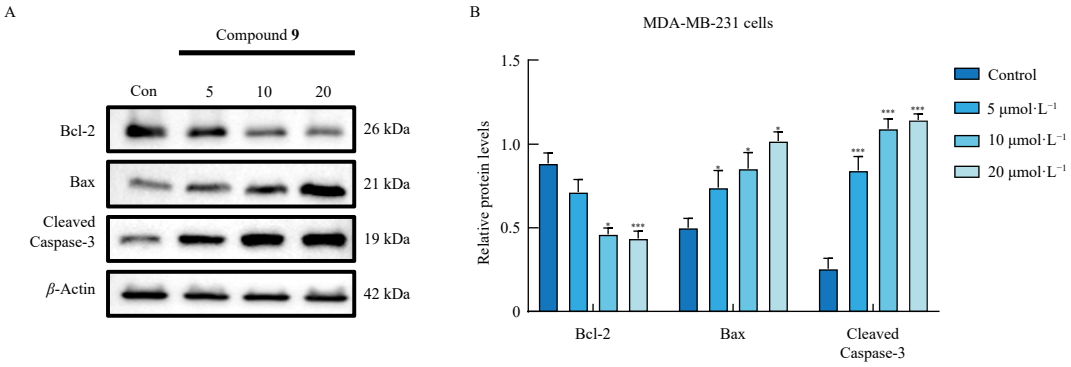

Fig. 7 Effect of compound **9** on the levels of apoptosis-associated molecules in MDA-MB-231 cells. (A) Levels of BAX, BCL-2, and Cleaved Caspase-3 in **9**-incubated MDA-MB-231 cells were examined using Western blotting. (B) Quantitative analysis of the protein levels indicated above. All data are represented as the average of three independent experiments ± SEM. $^{*}P < 0.05$; $^{***}P < 0.001$, *vs* control group.

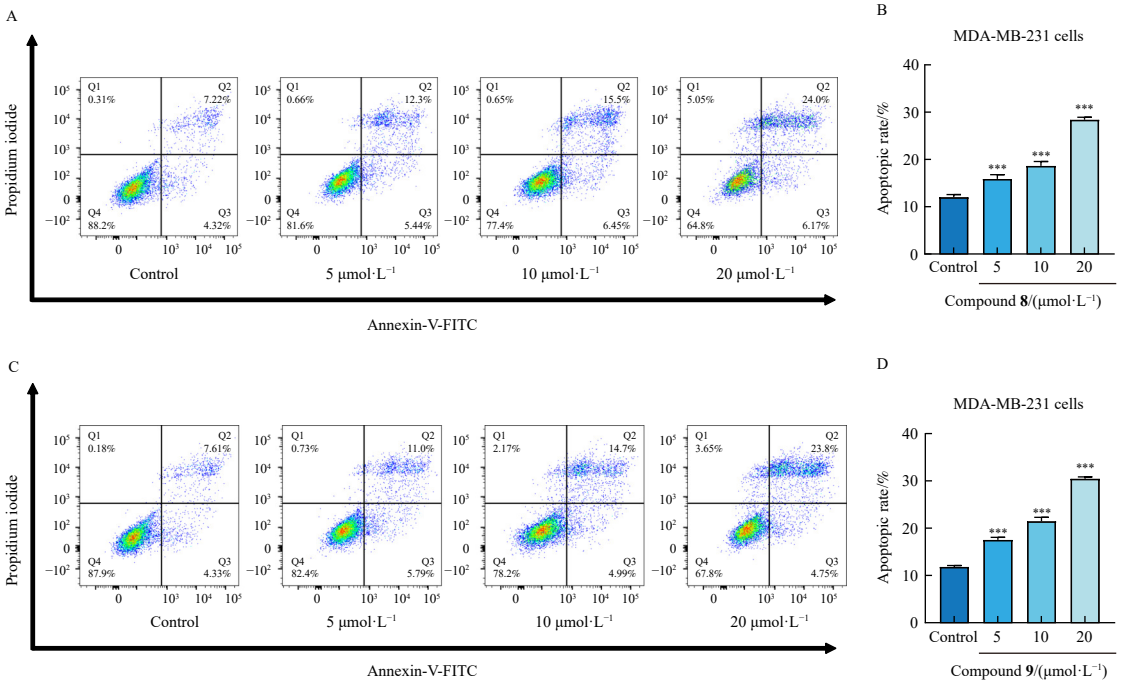

Fig. 8 MDA-MB-231 cells treated with **8** (A) and **9** (B) at 5, 10, and 20 μmol·L^{-1} for a duration of 48 h were stained using Annexin V-FITC/PI and immediately analyzed by flow cytometry. Quantitative analysis of the apoptosis rate of **8** (C) and **9** (D) treated levels. All data are represented as the average of three independent experiments ± SEM. $^{***}P < 0.001$, *vs* control group.

Table 3 Cytotoxic activities of compounds from *P. penangianum* in three cancer cell lines

Compd	IC_{50} ± SD (μmol·L^{-1})			Compd	IC_{50} ± SD (μmol·L^{-1})		
	$HepG_2$	MDA-MB-231	MCF-7		$HepG_2$	MDA-MB-231	MCF-7
1	> 80	> 80	60.12 ± 1.40	**8**	29.62 ± 3.57	7.93 ± 2.85	2.21 ± 1.38
2	42.48 ± 3.76	> 80	43.55 ± 4.65	**9**	28.34 ± 2.33	5.87 ± 1.58	3.52 ± 1.55
5	31.88 ± 1.59	> 80	> 80	**12**	> 80	> 80	55.27 ± 3.84
6	40.75 ± 2.88	> 80	39.02 ± 0.33	**14**	> 80	> 80	58.12 ± 3.47
Dox[a]	1.78 ± 0.11	1.91 ± 0.32	0.57 ± 0.25	**15**	> 80	> 80	50.59 ± 1.07

[a]Doxorubicin was used as positive controls. The compounds with IC_{50} values > 80 μmol·L^{-1} in the above 3 cell lines were not listed in the table. Values represent means ± SD of triplicate experiment.

Table 4 Inhibitory Effects of Compounds from *P. penangianum* on LPS-activated TNF-α, IL-6 and NO Production in RAW 264.7 Macrophages.

Compd.	IC_{50} ± SD (μmol·L^{-1})			Compd.	IC_{50} ± SD (μmol·L^{-1})		
	TNF-α	IL-6	NO		TNF-α	IL-6	NO
2	68.75 ± 0.85	25.77 ± 1.38	43.74 ± 2.97	**13**	43.50 ± 4.70	43.76 ± 3.27	61.84 ± 2.88
3	25.52 ± 1.02	20.51 ± 1.41	51.38 ± 3.81	**14**	28.12 ± 1.37	52.39 ± 3.59	50.54 ± 1.36
7	21.75 ± 0.81	23.41 ± 1.96	37.17 ± 4.11	**18**	31.52 ± 3.91	28.04 ± 2.19	52.99 ± 4.58
Dex[a]	13.35 ± 0.63	5.32 ± 0.56	14.72 ± 1.65				

[a]Dexamethasone was used as positive controls. The compounds with IC_{50} values > 80 μmol·L^{-1} were not listed in the table. Values represent means ± SD of triplicate experiment.

from Procell Life Science & Technology Co., Ltd (Wuhan, China). RAW 264.7 and MDA-MB-231 cells were cultivated in Dulbecco's Modified Eagle's Medium (DMEM) supplemented with 10% fetal bovine serum (FBS, Procell, Wuhan, China). MCF-7 and $HepG_2$ cells were maintained in MEM enriched with 10% FBS (Procell, Wuhan, China). All cell lines were incubated at 37 °C in a humidified atmosphere containing 5% CO_2.

Plant material. The *P. penangianum* plant was collected from Shimen City, Hunan Province, China, in December 2021. Dr. Wei Wang from the School of Pharmacy at Hunan University of Chinese Medicine, China, authenticated the specimen. A voucher specimen has been deposited in the TCM and Ethnomedicine Innovation & Development International Laboratory at Hunan University of Chinese Medicine, China (Accession number: 20211201).

Extraction and isolation. Air-dried powder of *P. penangianum* (100.0 kg) was extracted with 95% EtOH/water (H_2O), yielding a gummy crude extract (12.7 kg). A portion of the crude extract (6.0 kg) was suspended in water and then partitioned successively with ethyl acetate (EtOAc) to afford an EtOAc-soluble fraction (1.0 kg). The EtOAc-soluble fraction (0.5 kg) was separated through a macroporous resin column (EtOH/H_2O, 30 : 70, 50 : 50, 70 : 30, 95 : 5, *V/V*) to obtain four fractions (Fr. A–Fr. D). Fr. B (120.0 g) was subjected to silica gel column chromatography with a gradient of dichloromethane (CH_2Cl_2)/EtOAc/MeOH (1 : 0 : 0 to 0 : 1 : 0 to 0 : 1 : 1 to 0 : 0 : 1, *V/V*) to obtain sixteen fractions (Fr. B1-B16). and compounds **11** (6.0 g), **12** (40.0 mg), **9** (100.0 mg). Fr. B7 (2.3 g) was subjected to silica gel column chromatography with a gradient of CH_2Cl_2/MeOH (1 : 0 to 0 : 1, *V/V*) system to afford eleven fractions (Fr. B7.1–Fr.B 7.11), and compound **3** (5.0 mg) was isolated. Fr. B7.4 was then chromatographed on Sephadex LH-20 (MeOH, 100%), and six subfractions (Fr. B7.4.1–Fr. B7.4.6) were obtained. Fr. B7.4.3 was further purified by preparative HPLC (MeOH/H_2O, 68 : 32, 3 mL·min^{-1}), yielding compound **8** (11.9 mg, 17 min). Fr. B7.6 was purified by RP-C18 column chromatography (MeOH/H_2O, 35 : 65 to 100 : 0) to afford fifteen fractions (Fr. B7.6.1–Fr. B7.6.15). Fr. B7.6.7 was further purified by semi-preparative HPLC (MeOH/H_2O, 58 : 42, 3 mL·min^{-1}), resulting in compounds **13** (5.0 mg, 7.0 min) and **2** (3.8 mg, 9.0 min). Compound **1** (4.5 mg, 12.0 min) was obtained from Fr. B7.6.3 using preparative HPLC (MeOH/H_2O, 35 : 65 to 100 : 0, 3 mL·min^{-1}). Fr. B7.8 was purified by preparative HPLC (MeOH/H_2O, 58 : 42, 3 mL·min^{-1}), which resulted in compound **10** (6.0 mg, 10.0 min). Fr. B8 (3.8 g) was subjected to RP-C_{18} column chromatography with gradient elution (MeOH/H_2O, 35 : 65 to 100 : 0) to afford twenty-three fractions. Fr. B8.19 was further purified through preparative HPLC (Acetonitrile/H_2O, 50 : 50, 3 mL·min^{-1}), yielding compound **4** (10.0 mg, 13 min). Fr. B8.12 was loaded onto Sephadex LH-20 (MeOH, 100%) and purified by preparative HPLC (Acetonitrile/H_2O, 40 : 60, 3 mL·min^{-1}) to afford compound **7** (23.0 mg, 17 min). Fr. B10 (7.4 g) was chromatographically separated with RP C18 column (MeOH/H_2O, 30 : 70 to 100 : 0), which resulted in nineteen fractions. Fr. B10.7 was purified by preparative HPLC (MeOH/H_2O, 51 : 49, 3 mL·min^{-1}), which afforded compound **6** (82.0 mg, 24.8 min). Fr. B15 (15.2 g) was fractionated on an RP-C_{18} column (MeOH/H_2O, 30 : 70 to 100 : 0) to afford thirty-four fractions. Fr. B15.6 was subjected to a silica gel column (CH_2Cl_2/MeOH, 1 : 0 to 0 : 1,*V/V*) to obtain six subfractions. Fr. B15.6.5 was further purified by preparative HPLC (MeOH/H_2O, 50 : 50, 3 mL·min^{-1}) to yield compounds **16** (7.6 mg, 17.5 min), **17** (45.0 mg, 18.5 min), **18** (6.0 mg, 23.0 min), and **19** (5.0 mg, 25.0 min). Fr. B15.10 was fractionated using silica gel column chromatography with a gradient of CH_2Cl_2/MeOH (1 : 0 to 0 : 1, *V/V*) system to afford twenty fractions. Fr. B15.10.18 was further purified by preparative HPLC (MeOH/H_2O, 50 : 50, 3 mL·min^{-1}), which resulted in compounds **14** (18.3 mg, 18.2 min) and **15** (3.5 mg, 22.6 min). Fr. B15.15 was fractionated with Sephadex LH-20 (MeOH, 100%) and further purified using preparative HPLC (MeOH/H_2O, 60 : 40, 3 mL·min^{-1}), which yielded in compound **5** (5.0 mg, 12.0 min).

Jixueqioside A (**1**): Amorphous white powder, $[\alpha]_D^{20}$ −53 (*c* 0.06, CH_3OH); IR (KBr) V_{max} 3411, 1737, 1613, 1518, 1250, 1134 cm^{-1}; UV (MeOH) λ_{max} (log ε) 206 (4.59), 226 (4.33), 275 (3.81); ECD (MeOH) λ ($\Delta\varepsilon$) 242 (−1.5), 276 (−0.6); ^{1}H NMR (CD_3OD, 600 MHz) and ^{13}C NMR (CD_3OD, 150 MHz) data (Tables 1 and 2); HRESIMS *m/z* 511.1575 [M + Na]$^+$ (Calcd. $C_{25}H_{28}O_{10}Na^+$, 511.1580).

Jixueqioside B (**2**): Amorphous white powder; $[\alpha]_D^{20}$ +262 (*c* 0.10, CH_3OH); IR (KBr) V_{max} 3361, 1709, 1615, 1517, 1248, 1144 cm^{-1}; UV (MeOH) λ_{max} (log ε) 205 (4.45), 226 (4.17), 275 (3.61); ECD (MeOH) λ ($\Delta\varepsilon$) 242 (+0.4), 276 (+0.3); ^{1}H NMR (CD_3OD, 600 MHz) and ^{13}C NMR (CD_3OD, 150 MHz) data (Tables 1 and 2); HR-ESI-MS *m/z* 511.1575 [M + Na]$^+$ (Calcd. $C_{25}H_{28}O_{10}Na^+$, 511.1580).

Jixueqioside C (**3**): Amorphous white powder; $[\alpha]_D^{20}$ +40 (*c* 0.06, CH_3OH); IR (KBr) V_{max} 3426, 1733, 1616, 1516, 1457, 1249 cm^{-1}; UV (CH_3OH) λ_{max} (log ε) 206 (4.71), 226 (4.45), 275 (3.68); ECD (CH_3OH) λ ($\Delta\varepsilon$) 242 (+0.2), 276 (+0.1); ^{1}H NMR (CD_3OD, 600 MHz) and ^{13}C NMR (CD_3OD, 150 MHz) data (Tables 1 and 2); HR-ESI-MS *m/z* 501.1758 [M − H]$^-$ (Calcd. $C_{26}H_{29}O_{10}^-$, 501.1761).

Jixueqioside D (**4**): Colorless amorphous powder; $[\alpha]_D^{20}$ +35 (*c* 0.12, CH_3OH); IR (KBr) V_{max} 3461, 1633, 1630, 1517, 1464, 1291 cm^{-1}; UV (CH_3OH) λ_{max} (log ε) 228 (4.48), 290 (4.24); ECD (CH_3OH) λ ($\Delta\varepsilon$) 242 (+0.5), 276 (+1.2); ^{1}H NMR (CD_3OD, 600 MHz) and ^{13}C NMR (CD_3OD, 150 MHz) data (Tables 1 and 2); HR-ESI-MS *m/z* 473.1451 [M − H]$^-$(Calcd. $C_{24}H_{25}O_{10}^-$, 473.1448).

Jixueqioside E (**5**): White needles; $[\alpha]_D^{20}$ +150 (*c* 0.08, CH_3OH); IR (KBr) V_{max} 3454, 1725, 1642, 1517, 1421, 1249 cm^{-1}; UV (CH_3OH) λ_{max} (log ε) 205 (3.85), 226 (3.53), 275 (2.43); ECD (CH_3OH) λ ($\Delta\varepsilon$) 242 (+0.4), 276 (+0.2); ^{1}H NMR (CD_3OD, 600 MHz) and ^{13}C NMR (CD_3OD, 150 MHz) data (Tables 1 and 2); HR-ESI-MS *m/z* 687.2247 [M + Na]$^+$ (Calcd. $C_{32}H_{40}O_{15}Na^+$, 687.2265).

Jixueqioside F (**6**): Yellow powder; $[\alpha]_D^{20}$ +102 (*c* 0.08,

CH_3OH); IR (KBr) V_{max} 3412, 1612, 1515, 1463, 1249 cm^{-1}; UV (CH_3OH) λ_{max} (log ε) 203 (4.70), 226 (4.38), 275 (3.66); ECD (CH_3OH) λ ($\Delta\varepsilon$) 276 (+0.02); ^1H NMR (CD_3OD, 600 MHz) and ^{13}C NMR (CD_3OD, 150 MHz) data, see Tables 1 and 2); HR-ESI-MS *m/z* 461.1814 $[M - H]^-$ (Calcd. $C_{24}H_{29}O_9^-$, 461.1812).

Jixueqioside G (**7**): Colorless amorphous powder; $[\alpha]_D^{20}$ +118 (*c* 0.08, CH_3OH); IR (KBr) V_{max} 3407, 1738, 1611, 1515, 1249 cm^{-1}; UV (CH_3OH) λ_{max} (log ε) 203 (2.99), 226 (2.65), 273 (2.25); ECD (CH_3OH) λ ($\Delta\varepsilon$) 276 (+0.02); ^1H NMR (CD_3OD, 600 MHz) and ^{13}C NMR (CD_3OD, 150 MHz) data (Tables 1 and 2); HR-ESI-MS *m/z* 505.2051 $[M + H]^+$ (Calcd. $C_{26}H_{33}O_{10}^+$, 505.2074).

X-ray crystallographic analyses of 14. Compound **14** was crystallized from an H_2O–MeOH (2 : 3) solution at room temperature. The X-ray crystallographic data for **14** have been deposited in the Cambridge Crystallographic Data Centre, CCDC 2358984.

ECD calculations. The methodology for quantum chemical ECD calculations of compounds **1**–**7** is detailed in the Supporting Information.

Acid hydrolysis. The absolute configuration of the sugar moiety was determined by the HPLC method [11]. Compounds **1–7** (1.0 mg) underwent hydrolysis in 2 mol·L^{-1} HCl at 80 °C for 4 h, followed by extraction with EtOAc. The aqueous layer was neutralized, evaporated under vacuum, and dissolved in anhydrous pyridine (1.0 mL) containing L-cysteine methyl ester hydrochloride (2.0 mg). After heating the reaction mixture at 60 °C for 1 h, isothiocyanate (2.0 mg) was added, and the mixture was maintained at 60 °C for an additional hour. The reaction product was evaporated under vacuum, dissolved in MeOH, and analyzed *via* analytical HPLC [(Agilent ZORBAX Eclipse XDB-C18, 4.6 mm × 250 mm, 5.0 μm, USA); flow rate: 0.8 mL·min^{-1}; mobile phase: CH_3CN–0.06% aqueous formic acid (25 : 75, *V/V*); detection wavelength: 250 nm].

Cytotoxicity assays. The impact of the compounds on cell proliferation and viability was assessed using the cell counting kit-8 (CCK-8, Elabscience, China) assay. Cells were seeded in 96-well plates at a density of 8.0 × 10^3 cells/well in a final volume of 100 μL and exposed to varying concentrations (2.5, 5, 10, 15, 20, 40, 60, 80 μmol·L^{-1}) of the compounds. Following a 48-hour treatment period, 10 μL of CCK-8 solution was added to each well containing 100 μL of culture medium. The plate was then incubated at 37 °C for 0.5 h. Subsequently, the absorbance of each well was measured at 450 nm using a microplate reader (Biotek, USA).

Western blotting. Following 48 h of treatment with compounds **8** and **9** (5, 10, and 20 μmol·L^{-1}), the treated cells were harvested and lysed with RIPA buffer. The protein concentration of each sample was determined using the BCA Protein Assay Kit. Samples were diluted with 4 × loading buffer and denatured at 95 °C for 10 min. Subsequently, proteins were separated using 12.5% SDS-PAGE and transferred to PVDF membranes. The proteins on the membranes were then blocked in 5% nonfat milk–Tris-buffered saline-Tween 20 (TBST) solution at 25 °C for 2 h. The membranes were incubated with various primary antibody solutions overnight at 4 °C. Antibodies including anti-BAX (Cat. No. 50599-2-Ig), anti-BCL-2 (AF6139), anti-Cleaved Caspase-3 (AF7022), anti-Beclin 1 (AF5128), anti-LC3 (AF5402), and anti-PCNA (AF0239) were obtained from Proteintech (Wuhan, China) or Affinity (Jiangsu, China). Following incubation, membranes were washed four times with TBST solution (8 min each) and then incubated with the corresponding secondary antibodies. Finally, after incubation with an ECL chemiluminescence solution, protein bands on the membranes were visualized using a multispectral imaging system (Tanon 5200 Multi).

Flow cytometry staining. Following 48 h of sample treatment, cells were harvested, washed with cold PBS, and resuspended in 1× binding buffer. Each cell set underwent staining with annexin V-FITC and PI, followed by incubation at room temperature for 15 minutes. Flow cytometry analysis was subsequently conducted to assess cellular apoptosis.

4.2. Anti-inflammatory activity assays

Cell viability. RAW 264.7 cells were seeded at 8 × 10^3 cells/well in a 96-well plate and incubated overnight. The cells were then treated with compounds **1**–**19** (20 μmol·L^{-1}) for 24 h. Following the treatment period, CCK-8 solution (Elabscience, China) was added and incubated at 37 °C for 0.5 h. Subsequently, the absorbance was measured at 450 nm.

NO assay. RAW 264.7 cells were cultured at 2 × 10^4 cells/well in DMEM containing 10% FBS in 48-well plates for 24 h and subsequently pretreated with compounds **1**–**19** for 2 h prior to LPS (0.1 μg·mL^{-1}) (Beyotime, Shanghai, China) stimulation for 24 h. The supernatant of cultured cells was collected and combined with an equal volume of Griess reagent [equal volumes of 1% (*W/V*) sulfanilamide in 5% (*V/V*) H_3PO_4 and 0.1% (*W/V*) N-(1-naphthyl) ethylenediamine dihydrochloride], incubated at room temperature for 15 min, and the absorbance was measured at 540 nm using a microplate reader. Sodium nitrite ($NaNO_2$) served as a standard to calculate the nitrite concentration. Inhibition (%) was calculated as $(1-(A_{LPS\ +\ sample} - A_{untreated})/(A_{LPS} - A_{untreated}) \times 100$. The inhibition rates (%) were expressed as the mean ± standard deviation (SD) of at least three independent experimental determinations.

TNF-α and IL-6 assay. The quantification of TNF-α and IL-6 levels was conducted using a quantitative enzyme-linked immunosorbent assay (ELISA) kit (Elabscience, Wuhan, China). RAW 264.7 cells were cultured at 2 × 10^4 cells/well in DMEM supplemented with 10% FBS in 48-well plates for 24 h. Subsequently, the cells were pretreated with compounds **1**–**19** for 2 h and then stimulated with LPS (0.1 μg·mL^{-1}) for 24 h. The supernatant was then collected to assess the production of TNF-α and IL-6. Following the ELISA assay protocol, absorbance was measured at 450 nm. Cytokine concentrations were determined using a standard calibration curve. The half maximal inhibitory concentration (IC_{50}) values were calculated as the mean ± SD from at least three independent experimental determinations.

Statistical Analysis. Data obtained from breast cancer cells treated with compounds **8** and **9** were analyzed using a one-way ANOVA, performed with GraphPad Prism 9.5 software (GraphPad Software, San Diego, California, USA). Statistical significance was defined as $P < 0.05$.

Funding

This work was supported by the National Natural Science Foundation of China (No. 81874369), the Excellent Youth Project of the Hunan Provincial Department of Education (No. 22B0388), and the Project of Hunan Administration of Traditional Chinese Medicine (No. B2023143).

Declaration of competing interest

The authors declare that they have no known competing financial interests or personal relationships that could have appeared to influence the work reported in this paper.

References

1 Editorial Committee of Flora of China CAoS. Flora Reipublicae Popularis Sinicae(IV). Beijing: Science Press. 1990, P301-303.
2 Chen LF, Cai GX. Hunan Pharmacopoeia. Hunan Science and Technology Press. 2004, P2588-2589.
3 Zhou Q, Jian YQ, Yi P, et al. A comprehensive review on *Pronephrium penangianum*. *Isr J Chem*. 2019;59(5):371-377. https://doi.org/10.1002/ijch.201800141.
4 Luo Y, Jian YQ, Liu YK, et al. Flavanols from nature: a phytochemistry and biological activity review. *Molecules*. 2022;27(3):719. https://doi.org/10.3390/molecules27030719.
5 Tanaka N, Murakami T, Wada H, et al. Chemical and chemotaxonomical studies of filices. LXI. chemical studies on the constituents of *Pronephrium triphyllum* Hollt. *Chem Pharm Bull*. 1985;33(12):5231-5238. https://doi.org/

10.1248/CPB.33.5231.
6 Zhong XW, Zhang WX, Lu HX, et al. A new flavan-4-ol glycoside from *Pronephrium triphyllum*. *Chin Herb Med*. 2011;3(3):161-164. https://doi.org/10.3969/j.issn.1674-6384.2011.03.001.
7 Zhen F, Jing J, Lin CZ, et al. New flavanol glucosides from *Abacopteris aspera* (Presl) Ching. *Helv Chim Acta*. 2015;98(1):108-115. https://doi.org/10.1002/hlca.201400135.
8 Jiang JH, Tian L, Wang LQ, et al. Phenolic compounds from the fern *Glaphyropteridopsis erubescens* (Hook.) Ching. *Biochem Syst Ecol*. 2013;50:136-138. https://doi.org/10.1016/j.bse.2013.04.005.
9 Luo ZW, Yin FC, Wang XB, et al. Progress in approved drugs from natural product resources. *Chin J Nat Med*. 2024;22(3):195-211. https://doi.org/10.1016/S1875-5364(24)60582-0.
10 Zhao ZX, Ruan JL, Jin J, et al. Flavan-4-ol glycosides from the rhizomes of *Abacopteris penangiana*. *J Nat Prod*. 2006;69(2):265-268. https://doi.org/10.1021/np050191p.
11 Liu Y, Zhao JP, Chen Y, et al. Polyacetylenic oleanane-type triterpene saponins from the roots of *Panax japonicus*. *J Nat Prod*. 2016;79(12):3079-3085. https://doi.org/10.1021/acs.jnatprod.6b00748.
12 Chen J, Chen X, Lei YF, et al. Vascular protective potential of the total flavanol glycosides from *Abacopteris penangiana via* modulating nuclear transcription factor-κB signaling pathway and oxidative stress. *J Ethnopharmacol*. 2011;136(1):217-223. https://doi.org/10.1016/j.jep.2011.04.052.
13 Zhao ZX, Jin J, Ruan JL, et al. Antioxidant flavonoid glycosides from aerial parts of the fern *Abacopteris penangiana*. *J Nat Prod*. 2007;70(10):1683-1686. https://doi.org/10.1021/np0703850.
14 Tanaka N, Sada T, Murakami T, et al. Chemische und chemotaxonomische untersuchungen der pterophyten. XLV. chemische untersuchungen der inhaltsstoffe von *Glaphyropteridopsis erubescens* (Wall) Copel. *Chem Pharm Bull*. 1984;32(2):490-496. https://doi.org/10.1248/CPB.32.490.
15 Slade D, Ferreira D, Marais JP. Circular dichroism, a powerful tool for the assessment of absolute configuration of flavonoids. *Phytochemistry*. 2005;66(18):2177-2215. https://doi.org/10.1016/j.phytochem.2005.02.002.
16 Xie Q, Fan XM, Han YH, et al. Daphnoretin arrests the cell cycle and induces apoptosis in human breast cancer cells. *J Nat Prod*. 2022;85(10):2332-2339. https://doi.org/10.1021/acs.jnatprod.2c00504.
17 Lee SE, Sivtseva S, Lim C, et al. *Artemisia kruhsiana* leaf extract induces autophagic cell death in human prostate cancer cells. *Chin J Nat Med*. 2021;19(2):134-142. https://doi.org/10.1016/S1875-5364(21)60014-6.